



# Ab initio three-dimensional quantum dynamics of $\text{Ag}_3$ clusters in the NeNePo process

I. Andrianov<sup>a,b,\*</sup>, V. Bonačić-Koutecký<sup>c</sup>, M. Hartmann<sup>c</sup>, J. Manz<sup>a</sup>, J. Pittner<sup>c,d</sup>,  
K. Sundermann<sup>a,e</sup>

<sup>a</sup> *Institut für Chemie, Freie Universität Berlin, Takustraße 3, D-14195 Berlin, Germany*

<sup>b</sup> *National Academy of Sciences of Belarus, Institute of Physics, Skaryna Avenue 70, 220602 Minsk, Belarus*

<sup>c</sup> *Walther-Nernst-Institut für Physikalische und Theoretische Chemie, Humboldt-Universität zu Berlin, Bunsenstrasse 1, D-10117 Berlin, Germany*

<sup>d</sup> *J. Heyrovský Institute of Physical Chemistry, Academy of Sciences of the Czech Republic, Dolejskova 3, CZ-18223 Prague 8, Czech Republic*

<sup>e</sup> *Max-Planck Institut für Quantenoptik, Hans-Kopfermann-Straße 1, D-85748 Garching, Germany*

Received 17 August 1999; in final form 30 November 1999

## Abstract

The first three-dimensional quantum-dynamical ab initio simulation of the large amplitude vibrational dynamics of an  $\text{Ag}_3$  cluster initiated from its linear transition state is presented. This can be monitored by femtosecond pump-probe negative-ion to neutral-to-positive-ion spectroscopy with zero electron kinetic energy (NeNePo-ZEKE). The time evolution of the representative wavepacket confirms the dynamical effects which have been discovered previously by Wigner-type semiclassical simulations: the initial coherent bending and stretching from linear to near equilateral triangular configuration, followed by intracluster collision and intracluster vibrational relaxation with a weak fractional revival. In addition, the quantum wavepacket shows interferences and spreading. © 2000 Elsevier Science B.V. All rights reserved.

## 1. Introduction

Wolf et al. [1] (see also the extension [2]) pioneered NeNePo pump-probe femtosecond spectroscopy, also called charge reversal-spectroscopy [3], to investigate the timescale of the nuclear motion

of molecular systems in the ground electronic state. In their specific application, a nonequilibrium linear  $\text{Ag}_3$  cluster has been prepared by a one-electron photodetachment of linear  $\text{Ag}_3^-$ . The geometrical relaxation from the linear  $\text{Ag}_3$  to the triangular nuclear configuration has been investigated by a delayed ionizing probe pulse using two-photon ionisation. The one-photon photodetachment energy of the pump pulse was varied from 2.95 to 3.18 eV, while the two-photon probe pulse energy ranged

\* Corresponding author. Department of Chemistry, University College London, 20 Gordon Street, London WC1H 0AJ, UK. Fax: +44-171-380-7463; e-mail: andrian@chem123.chem.ucl.ac.uk

from 5.9 to 6.36 eV. (For structures and energetics of small neutral and charged  $\text{Ag}_n$  clusters, cf. Refs. [4,5]). An extension of the charge reversal technique using two-color excitation and sensitive ion and electron detection was also applied to the study of the  $\text{Ag}_3^-/\text{Ag}_3/\text{Ag}_3^+$  system by Boo et al. [3]. Recently, Leisner et al. presented the complementary experimental results, based on resonant two-photon excitation [6]. For a survey of these studies, see Ref. [7].

The original interpretation of the signals was based on the assumptions that the time-dependent Franck–Condon vibrational overlap integrals between the potential energy surfaces (PES) of  $\text{Ag}_3^-$  and  $\text{Ag}_3^+$  during the geometrical relaxation from the linear to the triangular equilibrium structure of  $\text{Ag}_3$  determine the shape of the signals. The model calculations [8,9] of the time-dependent ionization potential (IP) of  $\text{Ag}_3$ , which are based on a tight binding approximation for the PES, confirmed the drastic changes of the IP due to the geometrical relaxation.

Theoretical studies of the multi-state nuclear dynamics based on classical trajectories on the ground electronic adiabatic PES of  $\text{Ag}_3^-$ ,  $\text{Ag}_3$  and  $\text{Ag}_3^+$  (obtained from accurate ab initio quantum-chemistry calculations) and the simulations of the pump-probe femtosecond signals utilizing the Wigner representation of the vibrational density matrix by Hartmann et al. [10,11], elucidated the rich dynamics of this system. Moreover, they provided complementary information for the time-resolved experimental spectroscopy. In these studies it has been shown that the large amplitude dynamics of the  $\text{Ag}_3$  cluster initiated from the linear transition state involves, in addition to the configurational relaxation towards the triangular geometry, sequential intracluster vibrational relaxation (IVR) processes, which can dominate the intracluster dynamics. These processes involve intracluster collisions, the onset of IVR, resonant and dissipative IVR and vibrational equilibration, whose timescales were determined. Furthermore, their dependence on the initial cluster temperature was discussed. The simulations demonstrated that dissipative IVR and vibrational equilibration can be present in a three-atomic system at excess of vibrational energy of  $\approx 0.4$  eV corresponding to an equilibrium temperature of  $\approx 1400$  K. The calculated NeNePo-ZEKE signal and the total (integrated over the photoelectron energy (NeNePo)) signal showed how one

could identify the geometrical change, completion of IVR and vibrational coherence effects in the signals. The total NeNePo signals compared well with the available experimental data.

In order to investigate the quantum effects of the large amplitude dynamics, we present in this Letter the results of the first fully quantum-mechanical three-dimensional (3-D) simulations of the NeNePo-ZEKE process in  $\text{Ag}_3$  cluster based on the same ab initio adiabatic ground state PESs as used in Refs. [10,11]; for an ab initio 3-D simulation of the pump-probe investigation of small amplitude (in comparison with  $\text{Ag}_3$ ) dynamics of  $\text{Na}_3$  in the electronically excited B-state; see Refs. [12–14]. The quantum-dynamical approach allowed us complementary insight into the dynamics of the system in comparison with the semiclassical calculations of Hartmann et al. [10,11].

Even though the present ab initio quantum investigation has been stimulated by the experimental work [1,15,3], as well as by the previous semiclassical studies [10,11], a direct comparison is not applicable for two reasons. First, our simulation applies to a ZEKE scenario, which has not yet been verified experimentally. Second, we assume that the system has been prepared in a specific vibrational eigenstate of the anionic precursor, in contrast with the experimental thermal ensemble. Our simulations are thus designed to analyze the underlying molecular quantum dynamics in the experiments [1,15,3], and they should provide a touchdown for complementary, more demanding experiments.

## 2. Model and techniques

In our investigation, the vibrational dynamics of neutral Ag trimers, as induced by NeNePo spectroscopy [1,3], is simulated by the time evolution of a representative 3-D wavepacket. These three dimensions correspond to the normal modes of a trimer in the vicinity of the equilibrium  $D_{3h}$  equilateral triangular geometry. The modes considered are the symmetric stretch mode  $Q_s$ , the bending mode  $Q_x$ , and the asymmetric stretch mode  $Q_y$ . The potential energy surfaces for the  $\text{Ag}_3^-$ ,  $\text{Ag}_3^0$  and  $\text{Ag}_3^+$  of Refs. [10,11] were represented in terms of these normal modes.

The dynamics of the system was first investigated by solving the coupled time-dependent Schrödinger equations

$$i\hbar \frac{\partial}{\partial t} \begin{pmatrix} \Psi_A \\ \Psi_N \\ \Psi_C \end{pmatrix} = \begin{pmatrix} \hat{T} + V_{\hat{A}} & \hat{W}_{AN} & 0 \\ \hat{W}_{AN} & \hat{T} + V_{\hat{N}} & \hat{W}_{NC} \\ 0 & \hat{W}_{NC} & \hat{T} + V_{\hat{C}} \end{pmatrix} \begin{pmatrix} \Psi_A \\ \Psi_N \\ \Psi_C \end{pmatrix}, \quad (1)$$

where  $\Psi_i = \Psi_i(Q_x, Q_y, Q_s; t)$ ,  $i = A, N, C$  are the 3-D time-dependent wavefunctions moving on the PESs of the anion, neutral and cationic silver trimer respectively;  $\hat{T} = -\frac{\hbar^2}{2M}\Delta$  is the kinetic energy operator, where  $M = m_{\text{Ag}}$  is the mass of one silver atom;  $\hat{V}_i = \hat{V}_i(Q_x, Q_y, Q_s)$  is the potential energy;  $\hat{W}_j = -\mu_j \mathcal{E}(t)$ ,  $j = AN, NC$  is the electromagnetic field interaction term in electric dipole approximation, where  $\mu_j$  is the transition dipole moment (assumed to be independent on the nuclear coordinates) for the anion-neutral and neutral-cation transitions respectively;

$$\mathcal{E}(t) = \sum_{k=\text{pu,pr}} \mathcal{E}_k \exp\left[-\frac{(t-t_k)^2}{\sigma_k^2}\right] \cos(\omega_k t) \quad (2)$$

is the electric field. In the expression (2) we label two subsequent nonoverlapping pulses with Gaussian envelopes of (FWHM) widths  $\sigma_{\text{pu}}$ ,  $\sigma_{\text{pr}}$  centered at times  $t_k$ , carrier frequencies  $\omega_{\text{pu}}$ ,  $\omega_{\text{pr}}$ , and field strengths  $\mathcal{E}_{\text{pu}}$ ,  $\mathcal{E}_{\text{pr}}$  by pump (pu) and probe (pr), respectively. The time delay between the pump and probe laser pulses is  $t_d = t_{\text{pr}} - t_{\text{pu}}$ . In the following applications, the field strengths  $\mathcal{E}_{\text{pu}}$ ,  $\mathcal{E}_{\text{pr}}$  were chosen small enough so that the role of multiphoton processes during the pulse was negligible. The relative NeNePo signal is then independent on  $\mathcal{E}_{\text{pu}}$  and  $\mathcal{E}_{\text{pr}}$ . The coupled equations (1) correspond to simulations of NeNePo-ZEKE spectra, i.e. for zero kinetic energy of the photodetached electron. In the more general case of NeNePo spectra with arbitrary electron energies, the electronic continuum should be taken into account, see e.g. the one-dimensional model simulation in Ref. [16]. Application of such an approach to the present 3-D system this was prohibitively expensive for the available computer resources. Equations (1) were propagated in time using the split operator method [17], the timestep  $\Delta t$  being

equal to 0.24 fs, and the diagonalization of the Hamilton matrix at each timestep was avoided by using a modified integral equation approach, as in Ref. [18].

The procedure outlined above proved to be computationally demanding, so that only 2-D or a few 3-D calculations could be carried out, for exemplary choices of the laser parameters. For routine simulations of the NeNePo-ZEKE spectra, including systematic variations of the delay times, approximations had to be introduced. The optical excitation was treated using the quantum analog of the expression for the NeNePo-ZEKE signals from Ref. [10], to carry out a close comparison of quantum and semi-classical treatments. The pump pulse of zero duration ( $\sigma_{\text{pu}} = 0$ ) promotes the initial wavepacket from the anionic surface to that of a neutral unchanged, and the NeNePo signal scales with the density of the wavefunction accumulated in the Franck–Condon window of the probe pulse as follows:

$$S(t_d) \sim \sum_G \exp\left(-\frac{\sigma_{\text{pr}}^2}{\hbar^2} \{E_{\text{pr}} - V_{\text{NC}}(Q_x, Q_y, Q_s)\}^2\right) \times |\Psi_N(Q_x, Q_y, Q_s; t_d)|^2, \quad (3)$$

where  $S(t_d)$  is the NeNePo-ZEKE signal after (delay) time  $t_d$ ,  $E_{\text{pr}} = 2\hbar\omega_{\text{pr}}$  is the two-photon probe energy,  $V_{\text{NC}}$  is the energy gap between the cationic and neutral surface, and  $G$  is a predetermined set of grid points, over which the summation is performed. Variations of the widths of the pump pulse in the range 0–100 fs did not affect the resulting signal significantly, due to the slow motion of the heavy silver atoms after the preparation of the neutral cluster.

Using expression (3) to calculate the NeNePo-ZEKE spectra, the computational effort is significantly reduced, since it allows us to propagate the wavefunction only on the PES of neutral  $\text{Ag}_3$  instead of three coupled surfaces of (1). The approach was tested in two dimensions, by comparing the signals obtained from solving the system of equations (1) with the ones calculated with the 2-D analog of formula (3). The agreement between the two signals was very satisfactory. Details of the comparison will be reported elsewhere.

In our first, exemplary model simulation described here, the first excited vibrational eigenstate

Table 1  
Grid parameters for the propagation

Coordinate	Min ( $a_0$ )	Max ( $a_0$ )	Number of points
$Q_s$	2.5	6.5	256
$Q_x$	-7.0	1.5	256
$Q_y$	-1.3	1.3	128

of  $\text{Ag}_3^-$ , with energy of  $31 \text{ cm}^{-1}$  (corresponding to 57 K in units of kT), was chosen as an initial condition, in order to approach the lowest temperature of a canonical ensemble of trajectories from Ref. [10], i.e. 50 K. The vibrational eigenfunctions of the anion were computed using the direct relaxation method of Tal-Ezer and Kosloff [19]. An even more appropriate comparison, using density matrices representing the initial ensemble at 50 K, was computationally prohibitive.

The parameters of the 3-D spatial grid used for the propagation are summarized in Table 1. As seen from this table, the wavefunction has to be represented on a rather dense, albeit wide grid, in order to account for the large amplitude vibrational motion from the linear to the near equilateral triangle configuration. Also, the heavy mass of the silver atom (107.9 a.u.) means comparatively long timescales of nuclear wavepacket evolution. The grid size ( $256 \times 256 \times 128 = 8388608$  points) and the long propagation times required propagation programs adapted to a massively parallel supercomputer.

### 3. Results and discussion

The time evolution of the 3-D wavepacket on the  $\text{Ag}_3^0$  surface is presented in the Fig. 1 by projecting the total wavefunction on the  $Q_x$  and  $Q_s$  coordinates.

First, we observe the coherent motion of the wavepacket towards the region of equilibrium triangular geometry (Fig. 1a,b). This motion corresponds to the bending of the linear trimer, simultaneously accompanied by stretching and subsequent contraction. The asymmetric stretch mode does not play a significant role at this stage. A feature to note is the pronounced spreading behaviour of the wavepacket, in spite of some intuitive expectations that a heavy

molecule such as a silver trimer should behave ‘almost classically’, that is, the wavepacket should remain more localized during the propagation.

At the delay time of ca. 0.8 ps the leading portion of the wavepacket arrives at the region of the equilibrium triangular geometry, where it collides with a rather steep wall of the potential (Fig. 1c). This corresponds to the event which was discovered by means of classical trajectories in Ref. [10], and called ‘intracluster collision’. The bend cannot proceed any further, and the energy flows into the symmetric stretch mode, where a multi-nodal pattern of the wavefunction is formed due to interferences of parts of the wavepacket, which correspond to subsequent symmetric stretches and compressions, in close analogy to the classical trajectories in Ref. [10] (Fig. 1d).

After the intracluster collision, the remaining portion of the wavepacket arrives at the region of equilibrium triangular geometry, causing interference with the preceding partial wave and, therefore, creating complex nodal patterns. In addition, the energy starts to flow also into the asymmetric stretch mode, and we witness the onset of the intramolecular vibrational redistribution (cf. Fig. 1d,e).

As the IVR proceeds (Fig. 1e,f), the wavefunction gradually fills all available configuration space, and the kinetic energy of the wavepacket distributes equally among the three normal modes. The latter phenomenon was first found in [10], and confirmed in our quantum simulations (not shown here). Fig. 1f also shows that a small portion of the wavepacket flows back to the original configuration of the linear trimer – this fractional revival can also be seen in corresponding classical trajectories. The rather weak appearance of this recurrence in  $\text{Ag}_3$ , in contrast with the observation of fairly coherent revivals in other systems, in particular diatomic molecules [20–24], is a consequence of the resonant IVR invoked by the intracluster collision.

The quantum-dynamical simulation presented here thus complements the earlier semiclassical MD simulations [10], and allows us to establish the correspondence between quantal and classical descriptions of the same system. For comparison, in Fig. 2a an exemplary snapshot of the wavefunction at the time  $t = 1.2$  ps is presented together with the corresponding ensemble of classical trajectories of 1.2 ps duration (Fig. 2b).

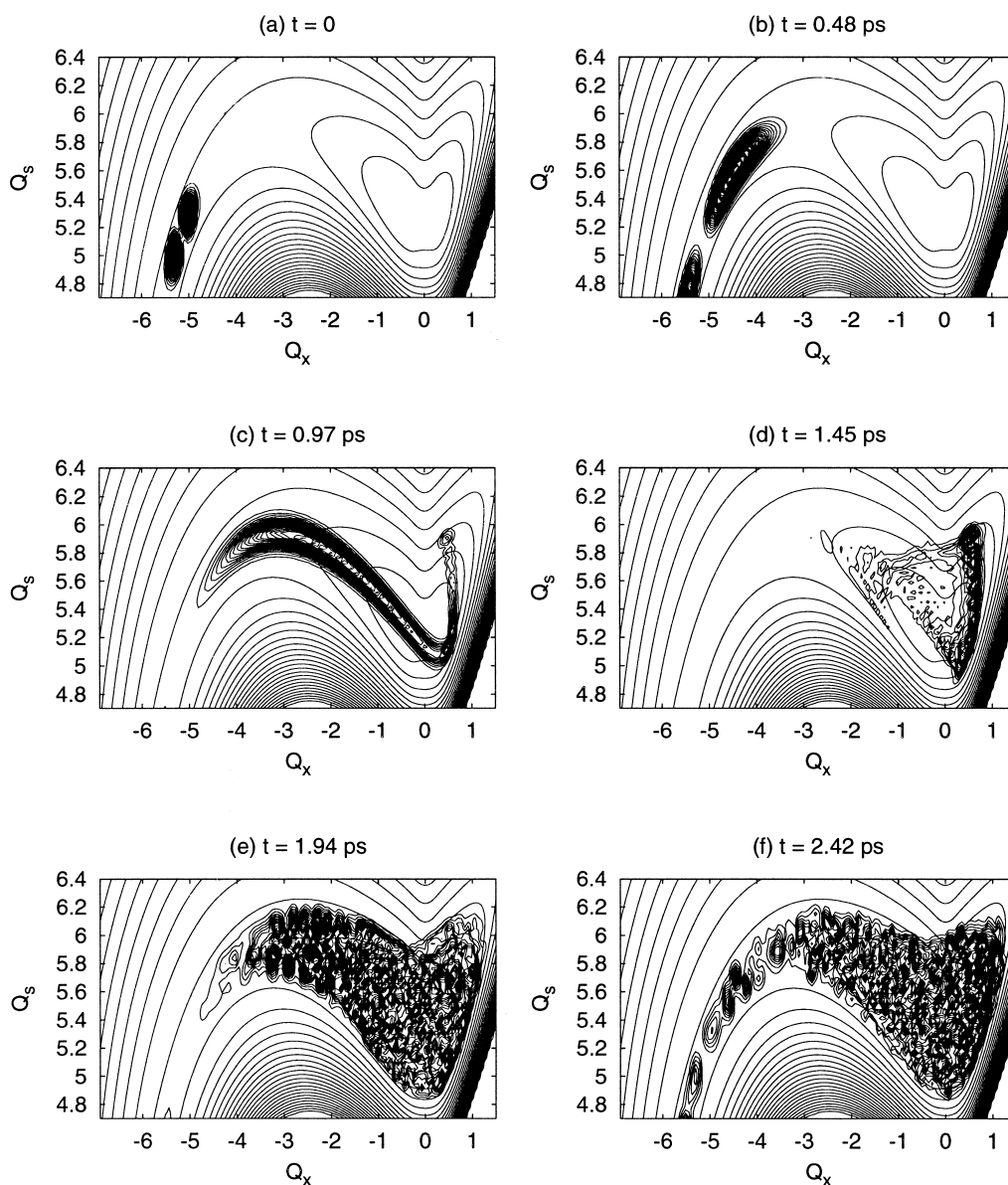


Fig. 1. Contour plots of the nuclear wavepacket projected on the  $(Q_s, Q_x)$  plane at several characteristic times, superimposed on equipotential contours of  $\text{Ag}_3^0$

We can see that the essential features attributed to the intracuster collision are present in both simulations. There are slight differences in the behavior of the classical trajectories and the quantal wavepacket, for example, the former rebound at a different region of the potential energy surface, but these differences

on the microscopic level do not influence the observables dramatically. A feature which is observed only in the quantum simulations is the very complex interference pattern of the 3-D wavefunctions, which originate from the superposition of a large number of eigenstates forming the initial wavepacket, which

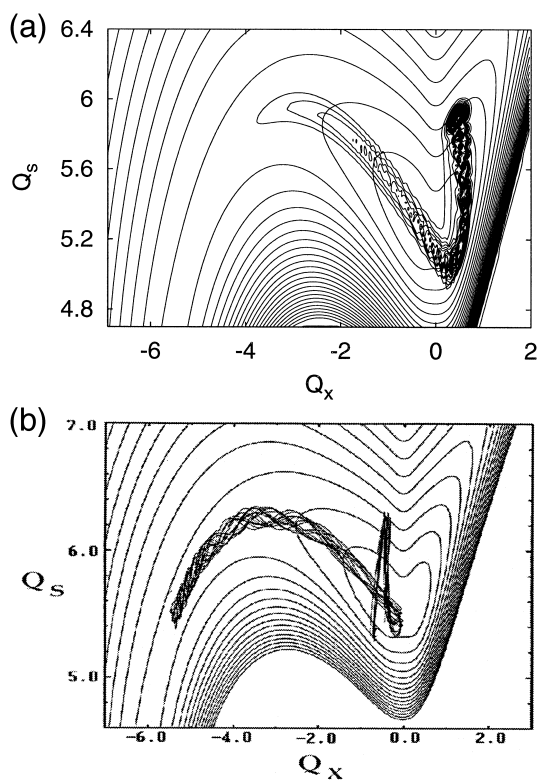


Fig. 2. Comparison between quantum-mechanical and semiclassical dynamics of  $Ag_3$ . (a) Quantum-mechanical wavepacket at  $t = 1.2$  ps, starting from the first vibrational excited state of  $Ag_3^-$ , with the average energy of 57 K. (b) Classical trajectories of 1.2 ps duration, starting from a canonical ensemble of  $Ag_3^-$  with 50 K initial temperature [10]

then evolve with phases due to slightly different energies. The resulting complex nodal pattern (Fig. 1e,f) corresponds to classical trajectories with apparently chaotic behaviour.

The resulting quantum-mechanical and semiclassical NeNePo-ZEKE spectra for three different frequencies of the probe laser pulse of 100 fs duration are compared in Fig. 3a,b respectively. The probe frequencies were chosen to probe the evolving wavepacket, or classical phase space density, at three characteristic domains on the potential energy surface during the evolution. The 6.5 eV probe samples the system in the vicinity of the linear geometry, the 5.8 eV pulse covers the region of triangular geometries, and the 6.1 eV value is chosen as an intermediate point.

The calculated semiclassical [10] and quantum NeNePo-ZEKE spectra exhibit common features, and are also in good quantitative agreement. The marginal differences between them, e.g. the slight shift of the quantum spectra towards the longer delay times, can be explained in terms of the different initial ensembles, with higher average kinetic energy in the semiclassical case. Also, the NeNePo-ZEKE spectra calculated quantum mechanically are noticeably broader than their semiclassical counterparts – this correlates with the wavepacket spreading. Both the semiclassical and quantum-mechanical results closely correspond to the experimental data of Refs. [1,3].

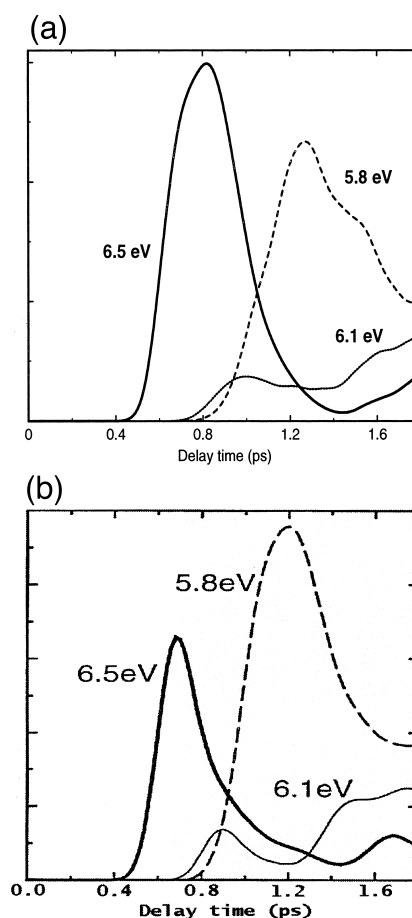


Fig. 3. Comparison of theoretical NeNePo-ZEKE spectra of  $Ag_3$  (arbitrary units) for different probe photon energies, obtained from quantum (a) and semiclassical (b) simulations adapted from Ref. [10] (see the text for a discussion).

#### 4. Conclusion

In this Letter the results of the first 3-D quantum-dynamical ab initio simulation of the NeNePo-ZEKE process in silver trimers have been presented. We have offered a detailed quantum-mechanical description of the molecular dynamics, including the large amplitude motion from the linear to the triangular configuration, followed by an intracluster collision, and the emergence as well as evolution of resonant IVR. In general, the quantum simulations confirm the mechanisms which have been discovered by applying the method of classical trajectories in Ref. [10]. Overall, the quantum and semiclassical results correspond to each other.

A more detailed study of the influence of the initial state on the dynamics of the system is in progress.

#### Acknowledgements

We are indebted to Prof. L. Wöste and Dr. T. Leisner for stimulating discussions and fruitful cooperation, and to Prof. R.H. Bisseling for his advice on wavepacket propagation on parallel computers. Generous financial support by Deutsche Forschungsgemeinschaft via Sfb 337 and Fonds der Chemischen Industrie is gratefully acknowledged. The computer simulations have been carried out on the Cray T3E supercomputer of Konrad-Zuse Zentrum für Informationstechnik, Berlin.

#### References

- [1] S. Wolf, G. Sommerer, S. Rutz, E. Schreiber, T. Leisner, L. Wöste, R.S. Berry, *Phys. Rev. Lett.* 74 (1995) 4177.
- [2] T. Leisner, S. Rutz, S. Vajda, S. Wolf, E. Schreiber, L. Wöste, in: A. Tramer (Ed.), *Fast Elementary Processes in Chemical and Biological Systems*, vol. 364, AIP Conference Proceedings, AIP Press, Woodbury, New York, 1996, pp. 603–620.
- [3] D.W. Boo, Y. Ozaki, L. Andersen, W. Lineberger, *J. Phys. Chem.* 101 (1997) 6688.
- [4] V. Bonačić-Koutecký, L. Češpiva, P. Fantucci, J. Koutecký, *J. Chem. Phys.* 98 (1993) 7981.
- [5] V. Bonačić-Koutecký, L. Češpiva, P. Fantucci, J. Pittner, J. Koutecký, *J. Chem. Phys.* 100 (1994) 490.
- [6] T. Leisner, S. Vajda, S. Wolf, L. Wöste, R.S. Berry, *J. Chem. Phys.* 111 (1999) 1017.
- [7] E. Schreiber, *Femtosecond Real-Time Spectroscopy of Small Molecules and Clusters*, Vol. 143, Springer Tracts in Modern Physics, Springer, Berlin, 1998.
- [8] H. Jeschke, M. Garcia, K. Bennemann, *Phys. Rev. A* 54 (1996) R4601.
- [9] H. Jeschke, M. Garcia, K.-H. Bennemann, *J. Phys. B.: At. Mol. Opt. Phys.* 29 (1996) L545.
- [10] M. Hartmann, J. Pittner, V. Bonačić-Koutecký, A. Heidenreich, J. Jortner, *J. Chem. Phys.* 108 (1998) 3096.
- [11] M. Hartmann, A. Heidenreich, J. Pittner, V. Bonačić-Koutecký, J. Jortner, *J. Phys. Chem. A* 102 (1998) 4069.
- [12] B. Reischl, *Chem. Phys. Lett.* 239 (1995) 173.
- [13] B. Reischl, R. de Vivie-Riedle, S. Rutz, E. Schreiber, *J. Chem. Phys.* 104 (1996) 8857.
- [14] R. de Vivie-Riedle, J. Gaus, V. Bonačić-Koutecký, J. Manz, B. Reischl, S. Rutz, E. Schreiber, L. Wöste, *Pulse Width Controlled Molecular Dynamics: Symmetric Stretch versus Pseudorotations in Na<sub>3</sub> (B)*, World Scientific, Singapore, 1996, pp. 319–326.
- [15] T. Leisner, Ch. Rosche, S. Wolf, F. Granzer, L. Wöste, *Surf. Rev. Lett.* 3 (1996) 1105.
- [16] O. Rubner, C. Meier, V. Engel, *J. Chem. Phys.* 107 (1997) 1066.
- [17] M.D. Feit, J.A. Fleck Jr., A. Steiger, *J. Comp. Phys.* 47 (1982) 412.
- [18] M.V. Korolkov, G.K. Paramonov, *Phys. Rev. A* 57 (1998) 4998.
- [19] H. Tal-Ezer, R. Kosloff, *Chem. Phys. Lett.* 127 (1986) 223.
- [20] I.S. Averbukh, N.F. Perelman, *Phys. Lett. A* 139 (1989) 449.
- [21] B.M. Garraway, K.-A. Suominen, *Rep. Prog. Phys.* 58 (1995) 365.
- [22] M.J.J. Vrakking, D.M. Villeneuve, A. Stolow, *Phys. Rev. A* 54 (1996) 1.
- [23] J. Heufelder, H. Ruppe, S. Rutz, E. Schreiber, L. Wöste, *Chem. Phys. Lett.* 269 (1997) 1.
- [24] S. Rutz, E. Schreiber, *Chem. Phys. Lett.* 269 (1997) 9.